Hindawi
Journal of Electrical and Computer Engineering
Volume 2023, Article ID 6623938, 16 pages
https://doi.org/10.1155/2023/6623938

Research Article

Spectral Efficiency Analysis for Uplink Multicell Massive MIMO Cellular Communication System under Fading Channels

Yibeltal Abebaw, Rajeev K. Shakya, Demissie Jobir Gelmecha, and Eshetu Tessema Ware

Department of Electronics and Communication Engineering, School of Electrical Engineering and Computing, Adama Science and Technology University, Adama, P.O. Box. 1888, Ethiopia

Correspondence should be addressed to Rajeev K. Shakya; rajeev.kumar@astu.edu.et

Received 24 June 2023; Revised 7 September 2023; Accepted 29 September 2023; Published 16 October 2023

Academic Editor: Jayshri Kulkarni

In multicell massive MIMO system, the maximum limit on area throughput can be achieved by improving spectral efficiency and cell density, as well as bandwidth. In order to evaluate the area throughput for such scenarios, the spectral efficiency (SE) that utilizes the linear zero forcing uplink combining scheme, can be modeled under the Rician fading channel and the BS in case of uplinks, is responsible to estimate the channel. Different from existing work, the proposed model incorporates various estimators such as minimum mean square error (MMSE), element-wise minimum mean square error estimators under Rician fading. The multicell scenarios with uplink (UL) massive MIMO has been analyzed using the proposed model under different cases such as pilot reuse factor, coherence block length, different number of antennas, and different estimators. The simulation results and analysis are presented based on these parameters. It is found that the average summation of SE per cell can be improved by optimizing MMSE channel estimation using ZF UL combiner, installing multiple BS antennas, serving multiple number of UEs per cell, and using efficient pilot reuse factor. The MMSE and ZF uplink combining are found to be more suitable in improving SE as compared to MMSE-MR. For example, the uplink SE of MMSE channel estimator for pilot reuse factors, 1, 3, and 4, is calculated as 22.5 bit/s/Hz/cell, 22.3 bit/s/Hz/cell, and 21 bit/s/Hz/cell, respectively. The uplink SE for EW-MMSE channel estimator with pilot reuse factors, 1, 3, and 4, is calculated as 22.5 bit/s/Hz/cell, 22 bit/s/Hz/cell, and 22 bit/s/Hz/cell, respectively. For the uplink SE of LS channel estimators, it can be 17.9 bit/s/Hz/cell, 20.2 bit/s/Hz/cell, and 20 bit/s/Hz/cell with pilot reuse factors as $f = 1$, 3, and 4, respectively. So, for $f = 3$, the maximum calculated uplink SE for MMSE, EW-MMSE, and LS is 17.6 bit/s/Hz/cell, 17.8 bit/s/Hz/cell, and 13 bit/s/Hz/cell, respectively. It can be concluded that the improved performance is obtained by reducing the pilot contamination at a pilot reuse factor $f = 3$ with different values of SNR, coherence block length, number of UEs, and number of BS antennas. There is also trade-off between the pilot contamination mitigation and the larger SE. However, there is not much effect on coherence block as when it increases, then the SE increases as well.

1. Introduction

Massive MIMO is one of the promising technologies for the next generation cellular systems. Each cell contains a central base station (BS) and many user equipment (UEs). Each base station contains a large number of antennas, approximately tens or hundreds of antennas that are used for communication with several single-antenna user equipment (UEs). The base station processes the signal using its antennas on both the uplink and downlink transmission sides [1, 2]. The MIMO technology is not new, and it already has a significant effect on both modern Wi-Fi networks and 4G LTE networks. Massive MIMO, on the other hand, is a recent improvement that was introduced for 5G new radio (NR) networks. The number of antenna elements and the multiuser capability within the antenna array are the two key features of massive MIMO technology that set it besides standard MIMO. To ensure future high traffic demand, we need to design and deploy a 5G network, which must enhance the performance of the network in terms of capacity, spectral efficiency (SE), energy efficiency, latency, network

security, and overall robustness [2, 3]. Due to the popularity of smart devices, the cellular network operators are facing challenges to satisfy the exponential traffic growth. To realize the attractive potential of massive MIMO system, a perfect match between the receiver and the actual channel is necessary, which can be best suitable for the cellular networks also [3–5]. In addition, the time division duplexing (TDD) mode is an outstanding choice for the operation of massive MIMO system. It can reduce the overhead of CSI acquisition by producing channel reciprocity, which means that the channel response is identical in both uplink and downlink transmission [6–10]. For cellular network scenarios, it can utilize available space resources, boosting channel capacity, and communication quality without requiring more spectrum resources and antenna transmission power [10–12], so that the need for new communication technology is motivated by the growing need for higher throughput in cellular wireless networks as well as the development of services such as the internet of things (IoT) and machine-to-machine communications (M2M). Hence, the MIMO technique can be a strong candidate to deliver high data rates in mobile networks and is a key enabler of modern cellular systems that offer less expensive ways to boost data rates, such as acquiring more bandwidth [11, 13, 14].

In terms of SE, one of the performance parameters is the area throughput that can be defined as an expression as $\text{Areathroughput} = B \times \text{Nc} \times \text{SE}$ [7, 9]. Here, B is the channel bandwidth; Nc is the number of cells in the unit area (cells per); and SE is the spectral efficiency per cell [3, 6, 8, 10]. So, the followings can be the criteria used to improve area throughput in massive MIMO system such as more (i) bandwidth allocation; (ii) cell density; and (iii) spectral efficiency. However, the more bandwidth allocation has limitation due to the use of limited frequency availability, and another is the increasing cell density that becomes difficult due to additional installations and configurations of base stations. So, the spectral efficiency (SE) improvement can only be a criterion for improving the area throughput [7].

In this article, the followings are the contributions by the motivations from the above observations: (i) the proposed model as ZF combiner that incorporates various estimators to analyze the SE of massive MIMO system under Rician fading channel. These include the minimum mean square error (MMSE), the element-wise minimum mean square error estimators; (ii) a detailed analysis is given based on ZF combiners with multicell scenario in different cases; (iii) the impact of pilot reuse factor with different base station antennas is studied in detail; (iv) the impact of coherence block length on uplink spectral efficiency of multicell massive MIMO system is also studied under different numbers of antennas and channel estimators.

The rest of the paper is organized as follows. The related work about massive MIMO system is described in Section 2. In Section 3, the proposed model design is described. The results analysis and conclusion remarks are covered in Section 4 and Section 5, respectively.

2. Related Works

In this section, the recent research work on multicell massive MIMO communication system based on different channels, estimators, antennas, line of sight (LOS), and nonline of sight (NLOS) is discussed. In [8], the authors had modeled a zero-forcing beam-forming scheme to improve spectral efficiency performance of the system. In [9], a Laplacian centralized scattering model was considered with a spatially correlated Rayleigh fading channel. The authors also included estimators such as a multicell minimum mean square error (M-MMSE) combining and precoding to handle the reduction on pilot contamination. Results claimed that the improved area throughput can be achieved with the M-MMSE technique, including the channel models such as the Laplacian-centralized scattering spatially correlated Rayleigh fading, one-ring scattering correlated Rayleigh fading, and uncorrelated Rayleigh fading [9]. In [13, 15], the pilot-based channel estimators were used to generate the channel state information of the desired system to optimize the pilot assignment. The authors had identified the pilot contamination using the pilot-assisted estimation, but they eliminated the channel estimated. Hence, the pilot contamination is avoided when there are no pilots. In [16, 17], the authors modeled a multicell MIMO system with favorable propagation conditions for a multicell massive MIMO network for the 5G cellular networks. They analyzed the SE performance on the effect of pilot contamination and several base station antennas. Three linear combiners were used in SE performance analysis, which includes the maximum ratio combiner (MRC), the zero-forcing (ZF), and the pilot-zero forcing (P-ZF) combiners. In their work, the drawback can be that a specified channel model is not considered to analyze spectral efficiency, so the impact of the line of sight path on SE performance for a multicell massive MIMO system cannot be observed. In [18], the spectral efficiency of a multiway massive MIMO system over a Rician fading channels is modeled for a single-cell massive MIMO system. However, there is no consideration of study on the effect of pilot contamination on spectral efficiency and the study with multicell massive MIMO was not considered in their methods. In [14], using Rician fading channel, the spectral efficiency analysis was also studied for the multicell massive MIMO system that is similar to references [19–23]. But, the only difference is that the results analysis is based on the linear maximal-ratio combining detector and Rician fading channel for different values of Rician factor and BS antennas. However, the authors did not consider the number of BS antennas and K-rice factors that are constantly growing unbound in case of the multicell massive MIMO system. A simple MMSE estimator can be used to eliminate the pilot contamination effects. In addition, the consideration of computational complexity in analysis should be studied as very much reasonable for spectral efficiency analysis. For both uplink and downlink, the authors in [25–27] had used a model for single user massive MIMO system for the improvement in BER with two retransmission schemes. However, their work is independent of the number of cells.

Different from this existing work, this article considers a multicell massive MIMO system with estimated channel state information at the receiver with three different types of channel estimators. The effect of pilot contamination on the SE performance is also studied for multicell massive MIMO scenario. Furthermore, the effect of line-of-sight and non-line-of-sight communication over Rician fading channels is also considered for better analysis. Our work includes the detailed analysis on the spectral efficiency with the pilot reuse factor, the number of users, the number of BS antennas, and the propagation condition of the system. Similar works given in [9, 19] were based on M-MMSE combining and precoding for the pilot contamination reduction and cell throughput improvements for massive MIMO multicell system. In our proposed design, the LS, MMSE, and EW-MMSE channel estimator and ZF combining techniques are analyzed to evaluate the pilot contamination effects and spectral efficiency performance.

3. The Proposed Model Design

In this section, a system model under TDD is described for a multicell massive MIMO system. In the process of developing a model of a multicell massive MIMO system, we choose and design channel models. The system model shown in Figure 1 considers the realism of a multicell massive MIMO system over Rician fading. In this TDD system, the multicell massive MIMO is assumed which shares the same time-frequency resources. All user equipment simultaneously occupy the available frequency-time resources for uplink pilot and data transmission.

The channel response h_{li}^{j} from users i in cell l to the BS within j_{th} cell is modeled as Rician fading channels as follows:

$$h_{li}^{j} = g_{li}^{j}\sqrt{\beta_{li}^{j}}, \tag{1}$$

where β_{li}^{j} is the large-scale fading coefficient, which contains the path loss and the shadowing effect of cellular environment and g_{li}^{j} is the small-scale fading; Here, the $g_{li}^{j} \in C^{M_j}$ are assumed to be complex Gaussian distribution with zero mean and unity variance, denoted by $\text{NC}(0, I_M)$.

The channel response between UE k in cell l and the base station in cell j is denoted by $h_{jk}^{j} \in \mathbb{C}^{M_j \times 1}$. Based on these training sequences, the desired base station can estimate the channels to the user equipment with some estimation error. The pilot sequence transmitted by user equipment is having a pilot length $\tau_p \geq k \approx \tau_p$ using TDD protocol [1]. In TDD mode, the channel response remains constant over a coherence block τ_c. The size of τ_c is determined by the carrier frequency and the external factor such as the propagation environment and UE mobility. It represents the number of orthogonal training sequences available for signaling with consideration of the same pilot sequences in each cell and k_{th} user in each cell has the same training sequences. To reduce interference in the transmission channel, a successful pilot assignment is a challenging task. Although it is necessary to assign more pilots for channel estimation in order to reduce pilot contamination, the spectral efficiency is declined when more resources within the coherence interval are assigned to pilots for estimation rather than the payload for transmission. As a resultant, when the number of users per cell increases, the number of pilot sequences also increases, and it leads to decreasing the spectral efficiency. Optimization on the resources is required for enhancing the spectral efficiency, since it allows more pilots to be assigned to data transmission rather than channel estimation [2]. In order to estimate the channel between user equipment (UE) of the different cell and the base station of desired cell channel, a model is designed as shown in Figure 1. It is only the system model for uplink multicell multiuser massive MIMO cellular network and the transmission process of uplink model. As shown in Figure 1, BS estimates the channel response from active UEs for making the efficient use of antennas.

Let ϕ_{jk} be the pilot sequence for k^{th} UE in j^{th} cell. The element of ϕ_{jk} is scaled by the uplink transmit power as $\sqrt{p_{jk}}$ and transmitted as the signal x_{jk} over τ_p uplink samples leading to the received uplink signal, denoted as $y_j^{\text{pilot}} \in \mathbb{C}^{M_j \times \tau_p}$ at BS j. At j^{th} BS, the received pilot signal can be expressed as follows:

$$\begin{aligned} y_j^{\text{pilot}} &= \sum_{k=1}^{K_j} \sqrt{p_{jk}} h_{jk}^{j} \phi_{jk}^{T} + \sum_{\substack{l=1,\\ L\neq j.}}^{L} \sum_{i=1}^{k_l} \sqrt{p_{li}} h_{li}^{j} \phi_{li}^{j} + n_j, \\ y_j^{\text{pilot}} &= \sqrt{p_{jk}} h_{jk}^{j} \phi_{jk}^{T} + \sum_{\substack{i=1,\\ i\neq k.}}^{k_j} \sqrt{p_{ji}} h_{ji}^{j} \phi_{ji}^{T} \\ &\quad + \sum_{\substack{l=1,\\ L\neq j.}}^{L} \sum_{i=1}^{k_l} \sqrt{p_{li}} h_{li}^{j} \phi_{li}^{j} + n_j^{\text{pilot}}, \end{aligned} \tag{2}$$

where y_j^{pilot} is denoted as j^{th} BS received pilot signal; $\sqrt{p_{jk}} h_{jk}^{j} \phi_{jk}^{T}$ is denoted as desired pilot signal; $\sum_{\substack{i=1\\ i\neq k}}^{k_j} \sqrt{p_{ji}} h_{ji}^{j} \phi_{ji}^{T}$ is denoted as intracell pilot signal; $\sum_{\substack{l=1\\ L\neq j}}^{L} \sum_{i=1}^{k_l} \sqrt{p_{il}} h_{li}^{j} \phi_{li}^{T}$ is denoted as intercell pilot; and n_j^{pilot} is denoted as AWGN.

In this model, for the sake of argument, from an arbitrary i^{th} UE in L^{th} cell, the BS j estimates the channel h_{li}^{j}. The BS is also multiplied or correlated y_j^{pilot} with this UE pilot sequence ϕ_{li} to generate the processed received pilot signal $y_j^{\text{pilot}} \in C^{M_j}$, which is given as follows:

$$\begin{aligned} y_j^{\text{pilot}} \phi_{li}^{\star} &= \sqrt{p_{jk}} h_{jk}^{j} \phi_{jk}^{T} \phi_{li}^{\star} + \sum_{\substack{i=1,\\ i\neq k.}}^{k_j} \sqrt{p_{ji}} h_{ji}^{j} \phi_{ji}^{T} \phi_{li}^{\star} \\ &\quad + \sum_{\substack{L=1,\\ l\neq j.}}^{L} \sum_{i=1}^{k_l} \sqrt{p_{il}} h_{li}^{j} \phi_{li}^{T} \phi_{li}^{\star} + n_j^{\text{pilot}} \phi_{li}^{\star}, \\ y_{jli}^{\text{pilot}} &= \sum_{\substack{L=1,\\ l\neq j.}}^{L} \sum_{i=1}^{k_l} \sqrt{p_{il}} h_{li}^{j} \tau_p + n_j^{\text{pilot}} \phi_{li}^{\star}. \end{aligned} \tag{3}$$

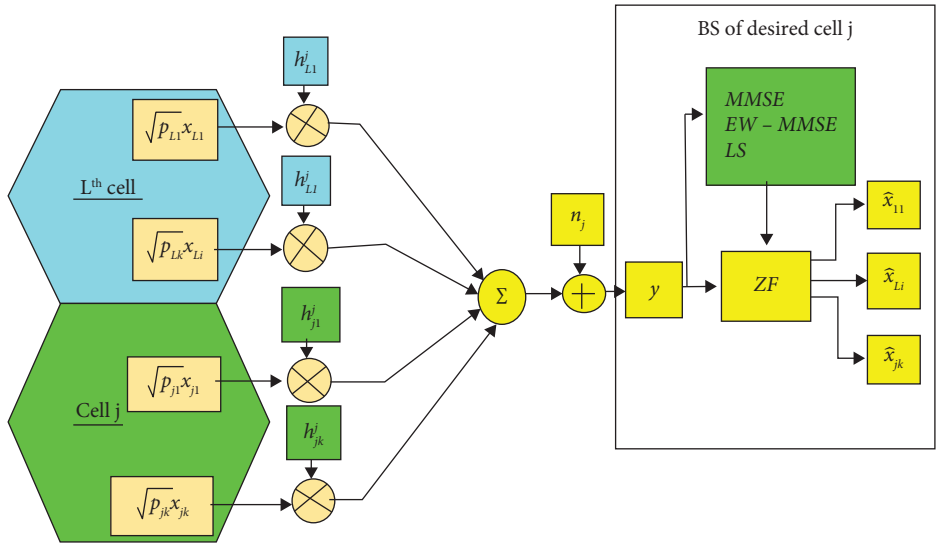

Figure 1: Uplink massive MIMO system model for multicell scenario.

To get the estimation of channel using the above-mentioned signal for the k^{th} user within the cell, a projection of y_j^{pilot} on ϕ_{jk}^{*} to obtain y_{jli}^{pilot} is as follows:

$$\begin{aligned} y_j^{\text{pilot}}\phi_{jk}^{*} &= \sqrt{p_{jk}}h_{jk}^{j}\phi_{jk}^{T}\phi_{jk}^{*} + \sum_{\substack{i=1,\\ i\neq k.}}^{k_j}\sqrt{p_{ji}}h_{ji}^{j}\phi_{ji}^{T}\phi_{jk}^{*} \\ &\quad + \sum_{\substack{L=1,\\ l\neq j.}}^{L}\sum_{i=1}^{k_l}\sqrt{p_{il}}h_{li}^{j}\phi_{li}^{T}\phi_{jk}^{*} + n_j^{\text{pilot}}\phi_{jk}^{*}, \\ y_{jjk}^{\text{pilot}} &= \sqrt{p_{ik}}h_{lk}^{j}\tau_p + n_j\phi_{jk}^{*}. \end{aligned} \tag{4}$$

Note that for all, $y_{jjk}^{\text{pilot}} = y_{jli}^{\text{pilot}}$, as $(l,i) \in \vartheta_{jk}$, because of the same pilot for all these UEs. Also, we have $n_j\phi_{jk}^{*} \backsim \text{NC}(0M_j\sigma_{ul}^2\tau_p I_{Mj})$.

When inside its own cell, there is possibility of strongest interference, the pilot assignment for the desired cellular network is important to utilize the desired pilot sequence efficiently. The value of ϑ_{jk} is given as follows:

$$\vartheta_{jk} = \left\{(l,i):\ \varnothing_{li} = \varnothing_{jk}, l = 1,\ 2,\ 3, \cdots, L\ \&\ i = 1,\ 2,\ 3, \cdots .K_l\right\}. \tag{5}$$

Considering the same pilot sequences for k^{th} user j^{th} cell, the $(l,i) \in \vartheta_{jk}$ implies the same, so $(j,k) \in \vartheta_{jk}$.

3.1. The Least Square (LS) Estimator. Assuming that from user equipment to base station, the transmitted data rate and the pilots are denoted by x. We have

$$y^{\text{pilot}} = h \star x, \tag{6}$$

where y^{pilot} is the received pilot signal, h is the unknown channel from UEs to BS antenna, and x denotes both the data rate and pilot length.

Using the received pilot signal, the estimation of the unknown channels from UEs to BS antennas is as follows:

$$h = y^{\text{pilot}} * \overline{x}. \tag{7}$$

In LS algorithm, only first-order statistics are assumed. In this algorithm, channel statistics are not considered beyond the first order. To estimate the unknown parameter h using an observed variable of $\widehat{y}^{\text{pilot}}$, we get

$$\widehat{h} = E\left\{\frac{\widehat{y}^{\text{pilot}}}{h}\right\}. \tag{8}$$

To estimate the desired channel between UEs and BS antennas of home cell using LS algorithm is as follows:

$$\widehat{h}_{jk}^{j(\text{LS})} = \frac{1}{\sqrt{p_{jk}}\tau_p} * y_{jjk}^{\text{pilot}}. \tag{9}$$

By substituting the value of y_{jjk}^{pilot}, the following is the simplified expression:

$$\widehat{h}_{jk}^{j(\text{LS})} = \frac{1}{\sqrt{p_{jk}}\tau_p} * \sqrt{p_{jk}}h_{jk}^{j}\tau_p + n_j\phi_{jk}^{*}. \tag{10}$$

If the desired cellular system-performing pilot is reused to increase the system capacity and to reduce pilot contamination, it simplifies the following expression:

$$\begin{aligned} \widehat{h}_{jk}^{j(\text{LS})} &= \frac{1}{\sqrt{p_{jk}}\tau_p}\left(\sqrt{p_{jk}}\,\tau_p h_{jk}^{j} + \sum_{(l,i)\in\vartheta_{jk}\setminus(j,k)}\sqrt{p_{li}}\,\tau_p h_{li}^{j} + n_j\phi_{jk}^{*}\right), \\ \widehat{h}_{jk}^{j(\text{LS})} &= \overline{h}_{\text{jk}}^{j} + \sum_{(l,i)\in\vartheta_{jk}\setminus(j,k)}\sqrt{\frac{p_{li}}{p_{jk}}}h_{li}^{j} + \frac{1}{\sqrt{p_{jk}}\tau_p} * n_j\phi_{jk}^{*}. \end{aligned} \tag{11}$$

3.2. Minimum Mean Square Error (MMSE) Estimator. The aim of any channel estimator is to estimate an unknown channel parameter h from observed pilot signals $\widehat{y}^{\text{pilot}}$. To find the value of estimated channel, the estimated value will be defined as $\widehat{h} = E\{h/\widehat{y}^{\text{pilot}}\}$. The aim of designing the MMSE channel estimator is to generate channel state information (CSI) at the receiver and minimize the error due to interference. So, the estimation $\widehat{h}$ is expressed as follows:

$$\begin{aligned}\text{MSE} &= J(\widehat{h})\\ &= E\{\|e\|^2\}\\ &= E\{\|h-\widehat{h}\|^2\}\\ &= E\{(h-\widehat{h})(h-\widehat{h})^H\}.\end{aligned} \tag{12}$$

The weighted vector W is used to find a better channel estimation. The W can be estimated in a better way using MMSE channel estimation by minimizing the MSE. According to orthogonality principle, the error on estimation, $e = h - \widehat{h}$, is orthogonal to $\text{LS}(\widehat{h})$ estimation. So, we obtain the following expression:

$$E\{e(\overline{h})^H\} = E\{(h-\widehat{h})\widehat{h}^H\}. \tag{13}$$

Finally, MMMSE channel estimation according to algorithm in [3] is given as follows:

$$H_{\text{MMSE}} = \widehat{h}_{li}^{j} = \widehat{h}_{li}^{j} + \sqrt{p_{li}}\tau_p R_{li}^{j}\psi_{li}^{j}\left(y_{jli}^{\text{pilot}} - \widehat{y}_{jli}^{\text{pilot}}\right), \tag{14}$$

where $\overline{y}_{jli}^{\text{pilot}} = \sum_{(l',i')\in p_{li}}\sqrt{p_{l'i'}}\overline{h}_{l'i'}^{j}$, $\psi_{li}^{j} = \tau_p \text{cov}(y_{jli}^{\text{pilot}})^{-1}$, and $\overline{h}_{li}^{j}$ is the mean corresponding to the LOS component.

3.3. Element-Wise-MMSE (EW-MMSE) Channel Estimator. The EW-MMSE channel estimator is a special type of MMSE channel estimators used to minimize the computational complexity of MMSE. It does not consider the spatial correlation matrix completely, but a diagonal element of the covariance matrix is considered. Based on literature [14], the complexity is found in calculation of MMSE estimation. So, using EW-MMSE, the reasonable performance can be obtained by minimizing the computational complexity of MMSE. According to [5], the EW-MMSE channel estimator is written as follows:

$$\widehat{\text{h}}_{li}^{j,\text{EW-MMSE}} = \overline{h}_{li}^{j} + \sqrt{p_{li}}D_{li}^{j}\wedge_{li}^{j}\left(y_{jli}^{\text{pilot}} - \overline{y}_{jli}^{\text{pilot}}\right), \tag{15}$$

where $D_{li}^{j} = \text{diag}(R_{li}^{j})$ and $\wedge_{li}^{j} = \text{diag}(\sum_{(l',i')\in p_{li}} p_{l'i'}\tau_p R_{l'i'} + \sigma^2 I_{mj})^{-1}$.

At j^{th} BS, the received signal during the uplink data transmission ($y_j \in C^{M_j}$) is defined as follows:

$$\begin{aligned}y_j &= \sum_{k=1}^{k_j} h_{jk}^{j}x_{jk} + \sum_{\substack{l=1,\\ l\neq j.}}^{L}\sum_{i=1}^{k_l} h_{li}^{j}x_{li} + n_j,\\ y_j &= \sqrt{p_{jk}}h_{jk}^{j}x_{jk} + \sum_{\substack{i=1,\\ i\neq k.}}^{k_j}\sqrt{p_{jk}}h_{jk}^{j}x_{jk} + \sum_{\substack{l=1,\\ l\neq j.}}^{L}\sum_{i=1}^{k_l}\sqrt{p_{li}}h_{li}^{j}x_{li} + n_j,\end{aligned} \tag{16}$$

where $n_j \in \text{Nc}(0_{mj}, \sigma_{ul}^2 I_{Mj})$ is the AWGN, the uplink data from k^{th} UE in L^{th} cell is $x_{lk} \in C$, and it has a power of $p_{lk} = E\{|x_{lk}|^2\}$.

3.4. Spectral Efficiency of the System. Spectral efficiency can be increased by using the radio network resources effectively that will result in increase of throughput. The most basic and common factors that control the spectral efficiency and throughput of cellular network are the signal to interference plus noise ratio (SINR) [24]. If the SINR of the network is not up to a limit, then the throughput degradation can happen. The BS can restore the original signal from data signal received from users to improve the SE. For this, a linear detector combination of ZF combining is used as follows:

$$v_{jk} = \widehat{h}_{jk}^{j}\left(\left(\widehat{h}_{jk}^{j}\right)^H\widehat{h}_{jk}^{j}\right)^{-1}, \tag{17}$$

where y_j is the desired signal from its k^{th} UE acting as interference. So, after doing the maximized ratio processing, the user signal can be expressed as follows:

$$\begin{aligned}\widehat{x}_{jk} &= v_{jk}^H y_j^{\text{uplink}}\\ &= \sqrt{p_{jk}}h_{jk}^{j}v_{jk}^H x_{jk} + \sum_{\substack{i=1,\\ i\neq k.}}^{k_j}\sqrt{p_{jk}}h_{jk}^{j}v_{jk}^H x_{jk}\\ &\quad + \sum_{\substack{l=1,\\ l\neq j.}}^{L}\sum_{i=1}^{k_l}\sqrt{p_{li}}h_{li}^{j}v_{jk}^H x_{li} + v_{jk}^H n_j.\end{aligned} \tag{18}$$

In general, we have the following expression:

$$v_{jk} = \widehat{h}_{jk}^{j}\left(\left(\widehat{h}_{jk}^{j}\right)^H\widehat{h}_{jk}^{j}\right)^{-1},$$

$$v_{jk} = \begin{cases}\dfrac{1}{\sqrt{p_{li}}\tau_p} * \left(\displaystyle\sum_{\substack{l=1\\ l\neq j}}^{L}\sum_{i=1}^{k_l}\sqrt{p_{li}}\,h_{li}^{j}\tau_p + n_j^{\text{pilot}}\phi_{li}^{*}\right)\text{LS},\\ \overline{h}_{jk}^{j} + \sqrt{p_{jk}}\,R_{jk}^{j}\psi_{jk}^{j}\left(y_{jli}^{\text{pilot}} - \overline{y}_{jli}^{\text{pilot}}\right)\text{MMSE},\\ \overline{h}_{jk}^{j} + \sqrt{p_{jk}}\,D_{jk}^{j}\Lambda_{jk}^{j}\left(y_{jli}^{\text{pilot}} - \overline{y}_{jli}^{\text{pilot}}\right)\text{EW}-\text{MMSE}.\end{cases} \tag{19}$$

Based on the above expressions, we analyze the achievable spectral efficiency of the uplink massive MIMO using these three different channel estimators. We have the signal $y_j^{\text{uplink}} \in C^{Mj}$ received at BS j and the uplink signal in cell L from user equipment k^{th} UE x_{jk}^{uplink}. As per literature [8, 21], the ergodic uplink capacity of k^{th} UE in cell j is lower bounded, and finally, we get the following expressions:

$$\begin{aligned}
\text{SE}_{jk}^{\text{uplink}} &= \frac{T_u}{T_c}\log_2\left(1+\text{SINR}_{jk}^{L}\right),\\
\text{SE}_{jk}^{ul,\text{MMSE}} &= \left(1-\frac{kf}{T_c}\right)\log_2\left(1+\frac{p_{jk}^2\tau_p tr\left(R_{jk}^j\psi_{jk}^j R_{jk}^j\right)+p_{jk}\left|\overline{h}_{jk}^j\right|^2}{\sum_{i=1}^{L}\sum_{i=1}^{k_l}p_{li}\delta_{li}^{ul}+\sum\limits_{(l,i)\in p_{jk}\setminus(j,k)}p_{li}\varsigma_{li}^{ul}-p_{jk}\zeta_{jk}^{ul}+\sigma_{ul}^2}\right),
\end{aligned} \tag{20}$$

where $\zeta_{jk}^{ul} = |\overline{h}_{jk}^j|^4/p_{jk}\tau_p tr\left(R_{jk}^j\psi_{jk}^j R_{jk}^j\right)+|\overline{h}_{jk}^j|^2$.

$$\begin{aligned}
\delta_{li}^{ul} &= \frac{p_{jk}\tau_p tr\left(R_{li}^j R_{jk}^j\psi_{jk}^j R_{jk}^j\right)+p_{jk}\tau_p\left(\overline{h}_{li}^j\right)^H R_{jk}^j\psi_{jk}^j R_{jk}^j\overline{h}_{li}^j+\left(\overline{h}_{li}^j\right)^H R_{li}^j\overline{h}_{jk}^j+\left|\left(\overline{h}_{jk}^j\right)^H\overline{h}_{li}^j\right|^2}{p_{jk}\tau_p tr\left(R_{jk}^j\psi_{jk}^j R_{jk}^j\right)+\left|\overline{h}_{jk}^j\right|^2},\\
\varsigma_{li}^{ul} &= \frac{p_{jk}p_{li}\left|R_{li}^j\psi_{jk}^j R_{jk}^j\right|^2+2\sqrt{p_{jk}p_{li}}\tau_{\text{p}}\text{Re}\left\{\text{tr}\left(R_{li}^j\psi_{jk}^j R_{jk}^j\left(\overline{h}_{jk}^j\right)^H\overline{h}_{li}^j\right)\right\}}{p_{jk}\tau_{\text{p}}\text{tr}\left(R_{jk}^j\psi_{jk}^j R_{jk}^j\right)+\left|\overline{h}_{jk}^j\right|^2},\\
\text{SE}_{jk}^{ul,\text{EW-MMSE}} &= \left(1-\frac{kf}{T_c}\right)\left(\frac{p_{jk}\left(p_{jk}\tau_p tr\left(D_{jk}^j\Lambda_{jk}^j D_{jk}^j\right)+\left|\overline{h}_{jk}^j\right|^2\right)^2}{\sum_{l=1}^{L}\sum_{i=1}^{k_l}p_{li}\mu_{li}^j-p_{jk}\left(p_{jk}\tau_p tr\left(D_{jk}^j\Lambda_{jk}^j D_{jk}^j\right)+\left|\overline{h}_{jk}^j\right|^2\right)^2+\sigma_{ul}^2\left(tr(\xi)+\left|\overline{h}_{jk}^j\right|^2\right)}\right),
\end{aligned} \tag{21}$$

where $\xi = p_{li}\tau_{\text{p}}D_{jk}^j\Lambda_{jk}^j D_{jk}^j(\psi_{jk}^j)^{-1}\Lambda_{jk}^j D_{jk}^j$.

4. Results and Discussion

In this section, the performance analysis of the proposed model is presented. A step-by-step procedure is described in flowchart as shown in Figure 2. The simulation parameters used for analysis are listed in Table 1.

$$\text{SE}_{jk}^{ul,f=1} = \left(1-\frac{k}{\tau_c}\right)\left(1+\frac{p_{jk}\left|E\left\{v_{jk}^H h_{jk}^j\right\}\right|^2}{\sum_{l=1}^{L}\sum_{i=1}^{kl}p_{li}E\left\{\left|v_{jk}^H h_{li}^j\right|^2\right\}-p_{jk}\left|E\left\{v_{jk}^H h_{jk}^j\right\}\right|^2+\sigma_{ul}^2E\left\{\left|v_{jk}\right|^2\right\}}\right), \tag{22}$$

$$\text{SE}_{jk}^{ul,f=3} = \left(1-\frac{3k}{\tau_c}\right)\left(1+\frac{p_{jk}\left|E\left\{v_{jk}^H h_{jk}^j\right\}\right|^2}{\sum_{l=1}^{L}\sum_{i=1}^{kl}p_{li}E\left\{\left|v_{jk}^H h_{li}^j\right|^2\right\}-p_{jk}\left|E\left\{v_{jk}^H h_{jk}^j\right\}\right|^2+\sigma_{ul}^2E\left\{\left|v_{jk}\right|^2\right\}}\right), \tag{23}$$

$$\text{SE}_{jk}^{ul,f=4} = \left(1-\frac{4k}{\tau_c}\right)\left(1+\frac{p_{jk}\left|E\left\{v_{jk}^H h_{jk}^j\right\}\right|^2}{\sum_{l=1}^{L}\sum_{i=1}^{kl}p_{li}E\left\{\left|v_{jk}^H h_{li}^j\right|^2\right\}-p_{jk}\left|E\left\{v_{jk}^H h_{jk}^j\right\}\right|^2+\sigma_{ul}^2E\left\{\left|v_{jk}\right|^2\right\}}\right). \tag{24}$$

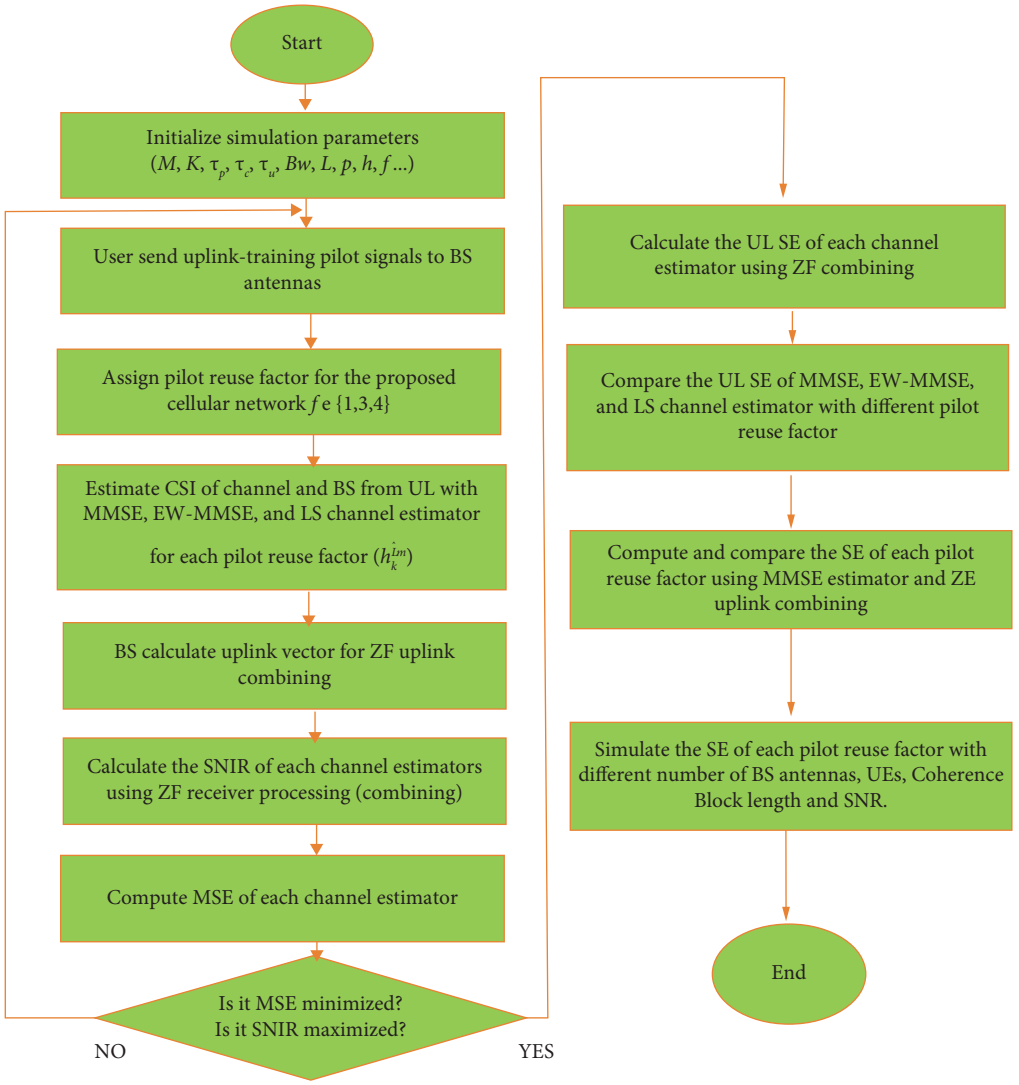

Figure 2: Flowchart for SE analysis for uplink multicell massive MIMO system.

Table 1: Simulation parameters.

Parameter description	Parameters
Cell type	Macro cell covers
Cell coverage area	$3\sqrt{3}/20.25^2$ km^2
UE to BS| separation distance	35 m
Carrier frequency	2 GHz
Linear detector	Zero forcing combining (ZF)
Channel estimators	MMSE, EW-MMSE, LS
Channel path loss model	Log-normal model
Path loss exponent	3.7 for urban environment
Number of cells	19
Number of BS antennas	$M \geq 100$
Pilot reuse factor	$f = 1, 2, 3$
Shadow fading standard deviation	$\sigma_{sf} = 4$ for LOS, $\sigma_{sf} = 10$ for NLOS
Number of UEs per cell	$k \geq 10$
Samples per coherence block	200, 300, 400, 500, 800
Uplink transmit power	0.1 Watt
Receiver noise power	−94 dB (thermal noise + noise figure
Channel gain at 1 km	−148.1 dBs
Bandwidth	20 MHz
Number of uplink pilot sequence	$\tau_p \geq k \approx \tau_p = k$ for universal pilot reuse $\tau_p = fk$ if pilot reuse factor is greater than one

Increasing the number of orthogonal pilot sequence is a straight forward way to decrease pilot contamination but it reduces the data rate; another mechanism is required to negotiate the pilot contamination problem and required data [13, 15, 18–20]. Pilot reuse factor is a mechanism to improve the required throughput by reducing the pilot contamination. The pilot reuse factor can be defined as $f = \tau_p/k$ as per TDD protocol. It also leads to SE performance improvement where f is the chosen integer and k denotes per cell number of UE. $f = 1$ is called as universal pilot reuse factor while $f > 1$ is named as nonuniversal pilot reuse factor. For analysis, three different pilot reuse factors are considered to evaluate the performance in equations (22)–(24) and are shown in Figure 3.

4.1. Effect of Different Pilot Reuse Factors and Number of BS Antennas at Different SNR Values on Uplink Spectral Efficiency of Multicell Massive MIMO Networks under Fading Channels. In Figure 4, the low SNR with BS antennas and its effect on the spectral efficiency are plotted for the multicell massive MIMO networks. In our proposed model with a BS antenna $M \in \{0 - 800\}$ having minimum SNR and users per cell, $k \geq 10$, the maximum SE is found to be 54 bit/s/Hz/cell with MMSE channel estimators and zero forcing uplink combining. As shown in Figure 4, the graph shows four times more SE. A pilot reuse factor $f = 3$ has a better spectral efficiency than other pilot reuse factors. Similarly, Figures 5(a) and 5(b) show the uplink spectral efficiency graph of multicell massive MIMO networks with different pilot reuse factors as a function of BS antenna numbers for 5 dB and 10 dB SNR. The graphs show the linear effect of the SNR and the BS antennas. In Figure 5, SE performance is improved than that of Figure 4 with SNR of 5 dB. For any value of SNR, BS, and antenna numbers, a pilot reuse factor $f = 3$ has higher spectral efficiency than other pilot reuse factors $f \in \{1, 4\}$.

Based on the above observations, MMSE estimator and ZF uplink combining indicate reasonable performance; for example, the proposed work using MMSE-ZE with a pilot reuse factor $f = 3$ has 58 bit/s/Hz/cell uplink spectral efficiency. This shows a great improvement of UL SE of a cellular network under the effect of shadowing and coherence interference.

As shown in Figures 4 and 5, the uplink SE averaged over a different number of BS antennas and shadow fading realization under high SNR and low SNR validate the theoretical results. As seen from figures, a pilot reuse factor $f = 3$ has better SE than the other two pilot reuse factors. Generally, increasing the number of BS antennas and SNR of the system yields a better SE. The potential pilot reuse factor $f = 3$ shows a maximum SE and a pilot reuse factor $f = 4$ also has a better performance than a universal pilot reuse factor, which is $f = 1$.

Table 2 shows the more detailed results of the uplink spectral efficiency of multicell massive MIMO cellular networks under fading environment.

4.2. Effect of Different Pilot Reuse Factors and Number of UEs at Different Coherence Block Lengths on Uplink Spectral Efficiency of Multicell Massive MIMO Networks under Rician Fading Channels. Here, we consider MR combining to detect the desired signal received from the estimated channels. Choosing a pilot reuse factor with MR combining is another way to reduce pilot contamination and improve the uplink spectral efficiency. In this analysis, the effect of the pilot reuse factor, coherence block, and number of UEs on the UL spectral efficiency over Rician fading channels is presented. Figures 6(a) and 6(b) show the uplink spectral efficiency of multicell massive MIMO systems vs the number of UEs within the cells for different pilot reuse factors with a coherence block length of $S = 400$ and $S = 500$. As shown in Figure 6(a), the spectral efficiency for pilot reuse factors $f \in \{3, 4\}$ is saturated for UEs ranging from 50 to 70, due to the presence of interference. For UEs, the ranges from 0 to 55 have improved SE as stated in IMT-advanced. The saturated SE for UEs ranging from 0 to 55 is 145, 181, and 155 for pilot reuse factors $f \in \{1, 3, 4\}$, respectively. As shown in Figure 7, pilot reuse factor $f = 3$ can improve the spectral efficiency of our desired systems with UEs up to 70.

As shown in Figure 6(b), the higher values of coherence block length make it easy to allocate the pilot sequences for channel estimation and uplink data transmission. As shown in Figure 6(b), a UE ranges from 0 to 40, and the maximum SE of each pilot reuse factor $f \in \{1, 3, 4\}$ is 125,135.5, and 150, respectively. However, for large number of users, still a universal pilot reuse factor $f = 1$ is dominant with higher spectral efficiency, while pilot reuse factors $f \in \{3, 4\}$ become minimum for higher number of UEs.

As shown in Figure 6, a cellular system with $k \leq 30$ and a pilot reuse factor $f = 3$ have a maximum SE than the other pilot reuse factors with different number of coherence block lengths. In order to design a particular network having a multicell and $k \leq 30$, $f = 3$ has a great role to improve the uplink SE and hence improvement in its area throughput, while a pilot reuse factor $f = 1$ has a linear effect on the uplink SE of multicell massive MIMO networks with an increased number of UE, especially for a UE $k > 30$. It is shown in Table 3 that as the number of user equipment are increased, the interference within a desired network will be increased. So, using a universal pilot reuse factor, $f = 1$ has a positive effect on the SE of multicell massive MIMO networks when we consider large number of users within desired cellular networks.

Table 3 shows the numerical results for Figures 7–9. It can show the effect of pilot reuse factors $f \in \{1, 3, 4\}$, code block length, and UEs on the uplink spectral efficiencies of multicell massive MIMO networks under fading channels. The table shows that a pilot reuse factor $f = 3$ for $k \leq 30$ and code block length $S \in \{200, 400, 500\}$ and $M = 1000$ have an enhanced uplink SE than $f = 1$ and $f = 4$. Furthermore, the SE performance with less number of UE is reasonable for $f = 4$ as compared to that of the pilot reuse factor $f = 1$.

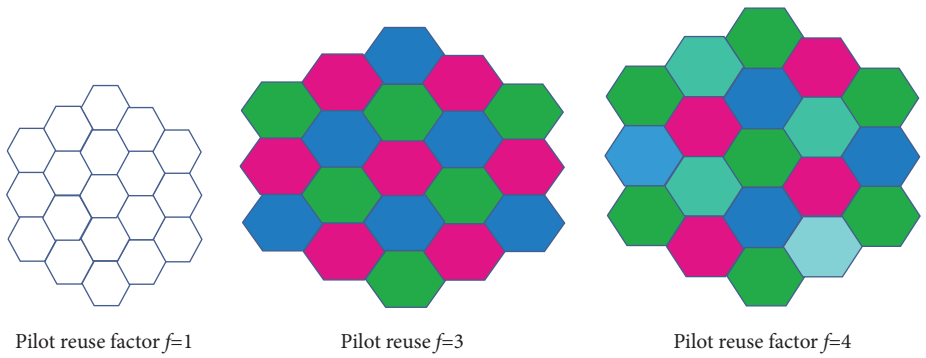

Figure 3: Pilot reuse factors for uplink multicell massive MIMO cellular networks.

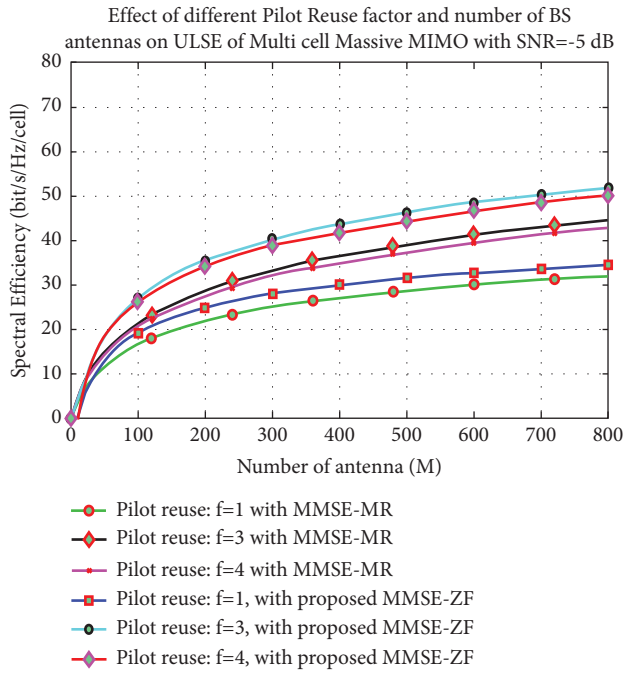

Figure 4: Uplink SE of multicell massive MIMO system under fading channels with different number of BS antennas and pilot reuse factor at SNR = −5 dB.

4.3. Effect of Different Pilot Reuse Factors and Number of BS Antennas Different UES on Uplink Spectral Efficiency of Multicell Massive MIMO Networks under Fading Channels. In this subsection, we consider pilot reuse factors with different number of users within a cell, which can efficiently enhance the spectral efficiency of multicell massive MIMO networks.

Figure 7 shows the uplink spectral efficiency of multicell massive MIMO networks under fading channels for different pilot reuse factors with varying BS antenna numbers with a UE of $k = 10$. In Figure 10, we consider BS antennas ranging from 0 to 1000 and UEs of $k = 10$ for three different pilot reuse factors of $f \in \{1, 3, 4\}$. As the graph indicates in Figure 10, a pilot reuse factor $f = 3$ has a greater potential to enhance the spectral efficiency of the overall system. It can be seen from the graph that the spectral efficiency with pilot reuse factor $f \in \{3, 4\}$ indicates little difference. So, these pilot reuse factors show the more efficient and maximum spectral efficiency with small number of users.

Figure 8 shows the corresponding spectral efficiency of our desired system for three different pilot reuse factors of $f \in \{1, 3, 4\}$ for UEs of $k = 20$ and $k = 35$ with coherence block length $\tau_c = 200$. As the number of users increase within the cell of a desired cellular network, the spectral efficiency of a universal pilot reuse factor $f = 1$ becomes maximal. In Figure 11, the spectral efficiency of pilot reuse factors $f \in \{1, 4\}$ has a little difference for less number of antennas. However, they have same spectral efficiency for higher number of BS antennas. A pilot reuse factor $f = 3$ still has a maximum spectral efficiency as compared with other pilot reuse factors. For UEs $k = 20$ and BS antennas ranging from 0 to 1000, the maximum spectral efficiency of different pilot reuse factors $f \in \{1, 3, 4\}$ becomes 60 bit/s/Hz/cell, 70 bit/s/Hz/cell, and

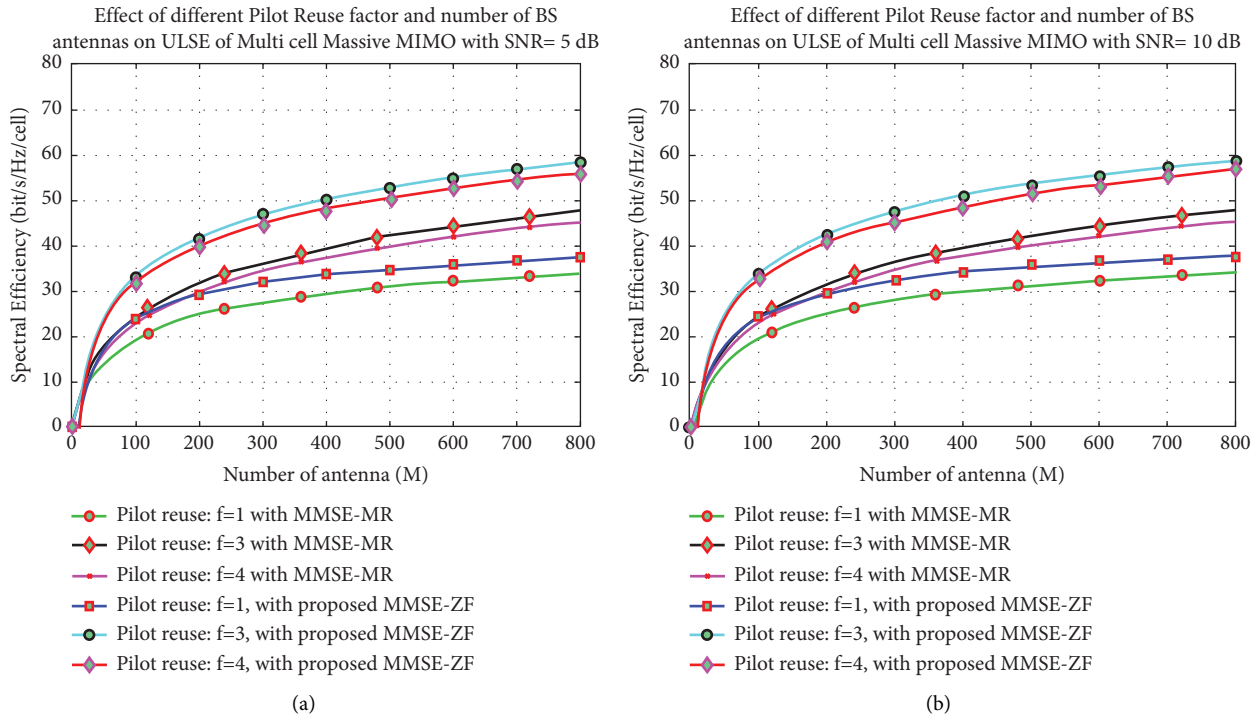

Figure 5: Uplink SE of multicell massive MIMO system under fading channels with different number of BS antennas and pilot reuse factor at (a) SNR = 5 dB and (b) SNR = 10 dB.

60 bit/s/Hz/cell, respectively. The parameters are given as $k = 35$, from 0 to 1000 range of BS antenna numbers and a coherence block length of 200 for three different pilot reuse factors $f \in \{1, 3, 4\}$. As shown in Table 4, the optimal spectral efficiency of these pilot reuse factors $f \in \{1, 3, 4\}$ is 87 bit/s/Hz/cell, 70 bit/s/Hz/cell, and 47 bit/s/Hz/cell, respectively.

4.4. Effect of Different Number of BS Antennas and UEs at Different Values of Coherence Block Length on Uplink Spectral Efficiency of Multicell Massive MIMO Networks under Fading Channels. The following figures show the effect of number of equipment and different BS antenna numbers and coherence block length. The value of coherence block length S depends mainly on mobility of users, frequency of operation, and propagation environment.

Figure 9 shows the uplink SE of multicell massive MIMO systems vs number of UEs under fading channels with a coherence block length of $S = 800$. As shown in figure, the number of BS antenna have a great potential to improve the SE of multicell massive MIMO networks. Due to the technique of spatial multiplexing between the UEs and BS antennas, the SE can be improved. The maximum uplink spectral efficiency of multicell massive MIMO network for different antenna numbers $M \in \{100, 200, 500\}$ is 55 bit/s/Hz/cell, 100 bit/s/Hz/cell, and 170 bit/s/Hz/cell, respectively.

As indicated in Table 5, for a coherence block length of $S = 500$, the maximum spectral efficiency for different number of BS antennas $M \in \{100, 200, 500\}$ is 45 bit/s/Hz/cell, 80 bit/s/Hz/cell, and 138 bit/s/Hz/cell, respectively. Generally, as the value of coherence block increases, the spectral efficiency also increases, as shown in Table 5.

4.5. Effect of Different Pilot Reuse Factors and Three Different Channel Estimators with Different Values of Coherence Block Length on Uplink Spectral Efficiency of Multicell Massive MIMO Networks under Fading Channels. In this subsection, we consider three different channel estimators with three different pilot reuse factors, for analyzing their spectral efficiencies with three different pilot reuse factors. At the receiver, we consider ZF combining used to detect the desired signals from desired users. As we discuss in the previous section, the channel is estimated by first sending pilot sequences from different users to BS antennas. BS estimates the channels between users and BS antennas.

Figure 10 shows the uplink spectral efficiency of multicell massive MMIMO network for MMSE and EW-MMSE LS with $f = 3$, using ZF uplink combining scheme. The uplink spectral efficiency of MMSE-ZF for a pilot reuse factor of $f = 3$ is 43.5 bit/s/Hz/cell. The uplink spectral efficiency of EW-MMSE-ZF for a pilot reuse factor of $f = 3$ is 35 bit/s/Hz/cell and the uplink spectral efficiency of LS-ZF with a pilot reuse factor of $f = 3$ is 35 bit/s/Hz/cell. This behaviour shows that the ZF uplink combining technique can suppress the coherence interference. As a resultant, the average sum spectral efficiency is enhanced with MMSE and $f = 3$ with ZF uplink combining.

Figure 11 shows the uplink spectral efficiency of multicell massive MMIMO network for MMSE and EW-MMSE LS with $f = 4$ using ZF uplink combining. The uplink spectral efficiency of MMSE-ZF for a pilot reuse factor of $f = 4$ is 37.5 bit/s/Hz/cell. The uplink spectral efficiency of EW-MMSE-ZF for a pilot reuse factor of $f = 4$ is 34.5 bit/s/Hz/cell and the uplink spectral efficiency of LS-ZF with a pilot reuse

Table 2: Effect of SNR and number of BS antennas on SE of multicell massive MIMO over fading channels.

S. No.	SNR values	Maximum SE at $f=1$ with proposed MMSE-ZF	Maximum SE at $f=3$ with proposed MMSE-ZF	Maximum SE at $f=4$ with proposed MMSE-ZF	Maximum SE at $f=1$ with MMSE-MR	Maximum SE at $f=3$ with MMSE-MR	Maximum SE at $f=4$ with MMSE-MR
1	−5 dB	36 bit/s/Hz/cell	54 bit/s/Hz/cell	50 bit/s/Hz/cell	32 bit/s/Hz/cell	44 bit/s/Hz/cell	42 bit/s/Hz/cell
2	5 dB	36 bit/s/Hz/cell	58 bit/s/Hz/cell	56 bit/s/Hz/cell	33 bit/s/Hz/cell	46 bit/s/Hz/cell	44 bit/s/Hz/cell
3	10 dB	38 bit/s/Hz/cell	60 bit/s/Hz/cell	58 bit/s/Hz/cell	35 bit/s/Hz/cell	48 bit/s/Hz/cell	46 bit/s/Hz/cell

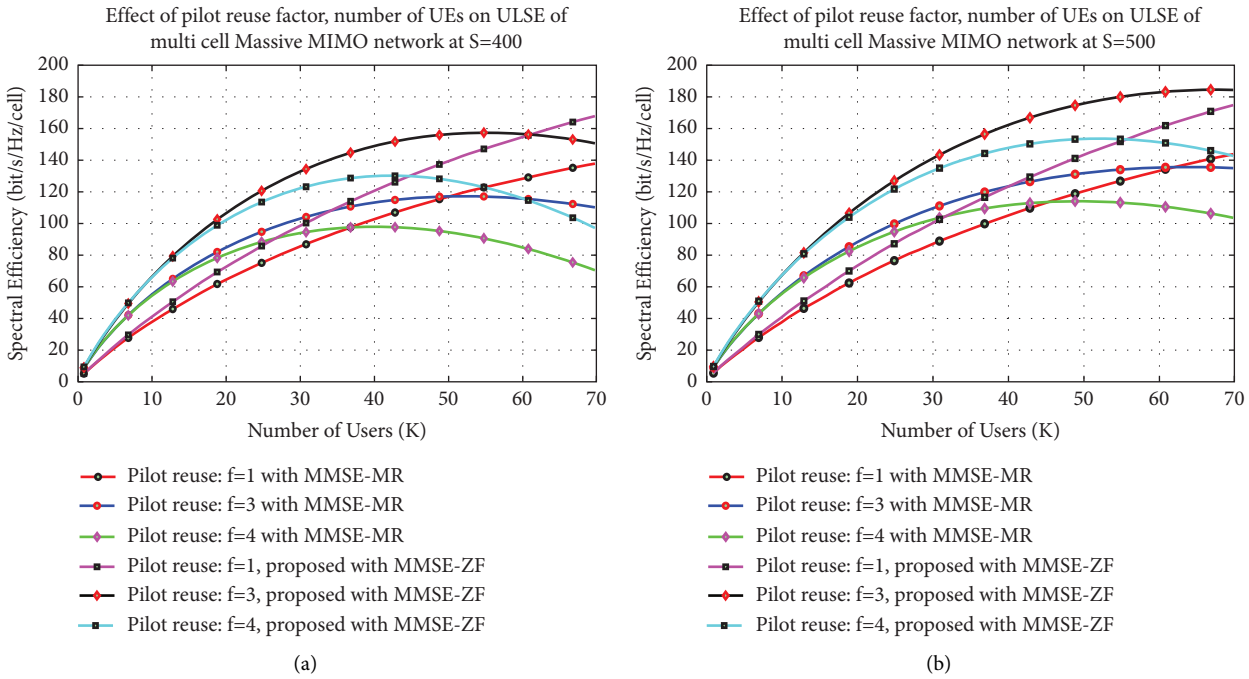

Figure 6: Uplink SE of multicell massive MIMO system under fading channels with different number of users and different pilot reuse factors at coherence block length of (a) $S = 400$ and (b) $S = 500$.

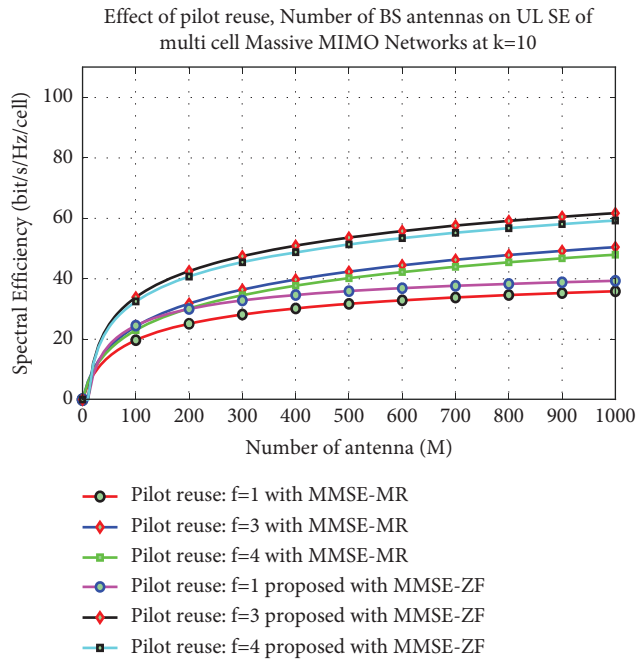

Figure 7: Effect of different pilot reuse factors and number of BS antennas on the uplink SE of multicell massive MIMO network under fading channels at $k = 10$.

factor of $f = 1$ is 34.5 bit/s/Hz/cell. As a resultant, still MMSE channel estimation technique is better to suppress the coherence interference and to enhance the uplink spectral efficiency of multicell massive MIMO system for $f = 4$. Using ZF linear uplink combiner is better to suppress the coherence interference.

Table 3: Effect of code block length and UEs on SE of multicell massive MIMO system under fading channels.

	Maximum SE (bit/s/Hz/cell) when $K \leq 30$ with proposed MMSE-ZF			Maximum SE (bit/s/Hz/cell) when $K > 30$ with proposed MMSE-ZF			Maximum SE (bit/s/Hz/cell) when $K \leq 30$ with MMSE-MR			Maximum SE (bit/s/Hz/cell) when $K > 30$ with MMSE-MR		
	$f=1$	$f=3$	$f=4$	$f=1$	$f=3$	$f=4$	$f=1$	$f=3$	$f=4$	$f=1$	$f=3$	$f=4$
$S=200$	68	98	78	135	≈0	≈0	65	75	60	110	≈0	≈0
$S=400$	125	150	135	155	150	100	85	100	90	140	118	100
$S=500$	145	181	155	170	181	155	80	115	100	140	138	115

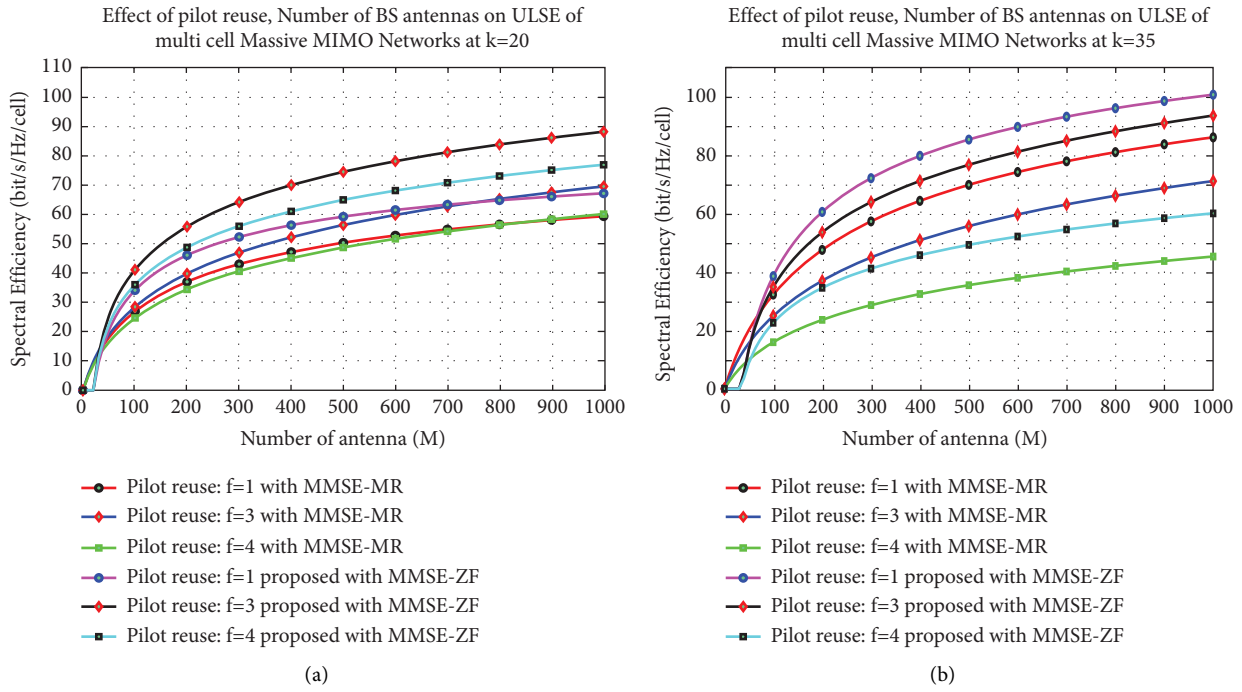

Figure 8: Effect of different pilot reuse factors and number of BS antennas on the uplink SE of multicell massive MIMO network under fading channels at (a) $k=20$ and (b) $k=35$.

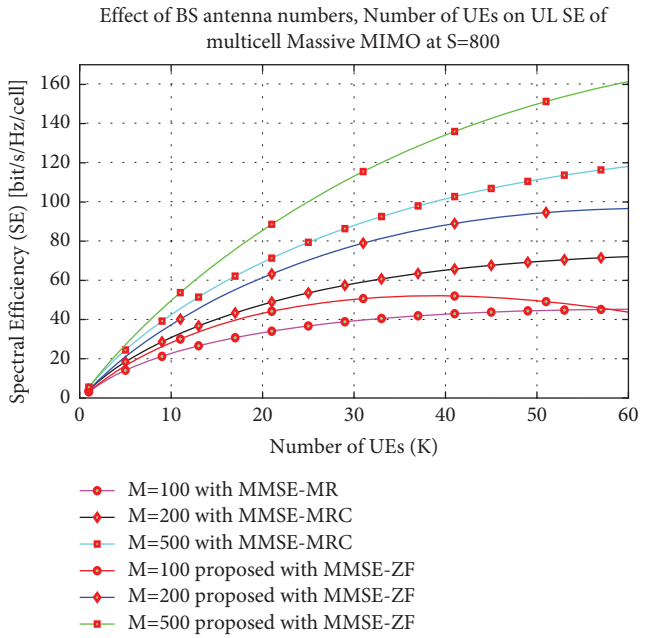

Figure 9: Uplink SE of multicell massive MIMO system under fading channels VS number of UEs with different number of BS antennas at coherence block of $S=800$.

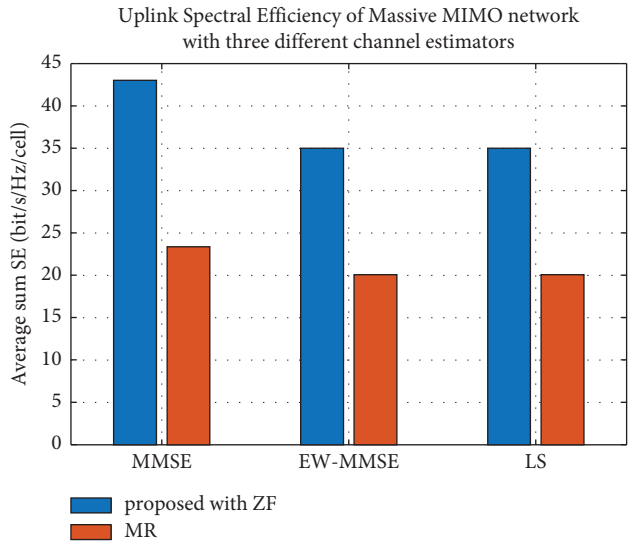

Figure 10: Average sum SE of multicell massive MIMO network for MMSE and EW-MMSE LS with $f = 3$, using ZF uplink combining scheme.

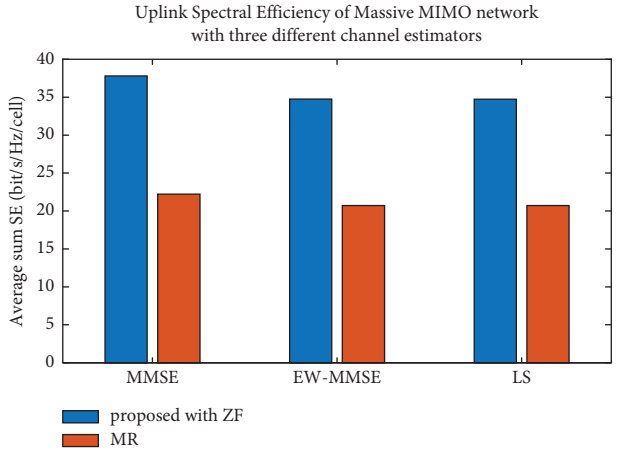

Figure 11: Average sum SE of multicell massive MIMO network for MMSE and EW-MMSE LS with $f = 4$ using ZF uplink combining.

Table 4: Numerical results of uplink spectral efficiency of three different pilot reuse factors.

	Maximum uplink spectral efficiency for different pilot reuse factors with proposed MMSE-ZF			Maximum uplink spectral efficiency for different pilot reuse factors with proposed MMSE-MR		
Number of users	$f = 1$	$f = 3$	$f = 4$	$f = 1$	$f = 3$	$f = 4$
$K = 10$	38 bit/s/Hz/cell	64 bit/s/Hz/cell	60 bit/s/Hz/cell	38 bit/s/Hz/cell	50 bit/s/Hz/cell	48 bit/s/Hz/cell
$K = 20$	70 bit/s/Hz/cell	90 bit/s/Hz/cell	78 bit/s/Hz/cell	60 bit/s/Hz/cell	70 bit/s/Hz/cell	60 bit/s/Hz/cell
$K = 35$	100 bit/s/Hz/cell	90 bit/s/Hz/cell	60 bit/s/Hz/cell	85 bit/s/Hz/cell	75 bit/s/Hz/cell	45 bit/s/Hz/cell

Table 5: Effect of code block length, UE, and BS antenna on SE under fading channels.

	Maximum SE at $M = 100$ with proposed MMSE-ZF	Maximum SE at $M = 200$ with proposed MMSE-ZF	Maximum SE at $M = 500$ with proposed MMSE-ZF	Maximum SE at $M = 100$ with proposed MMSE-MR	Maximum SE at $M = 200$ with proposed MMSE-MR	Maximum SE at $M = 500$ with proposed MMSE-MR
$S = 400$	35 bit/s/Hz/cell	70 bit/s/Hz/cell	115 bit/s/Hz/cell	35 bit/s/Hz/cell	55 bit/s/Hz/cell	85 bit/s/Hz/cell
$S = 500$	45 bit/s/Hz/cell	80 bit/s/Hz/cell	138 bit/s/Hz/cell	40 bit/s/Hz/cell	60 bit/s/Hz/cell	100 bit/s/Hz/cell
$S = 800$	55 bit/s/Hz/cell	100 bit/s/Hz/cell	170 bit/s/Hz/cell	45 bit/s/Hz/cell	75 bit/s/Hz/cell	120 bit/s/Hz/cell

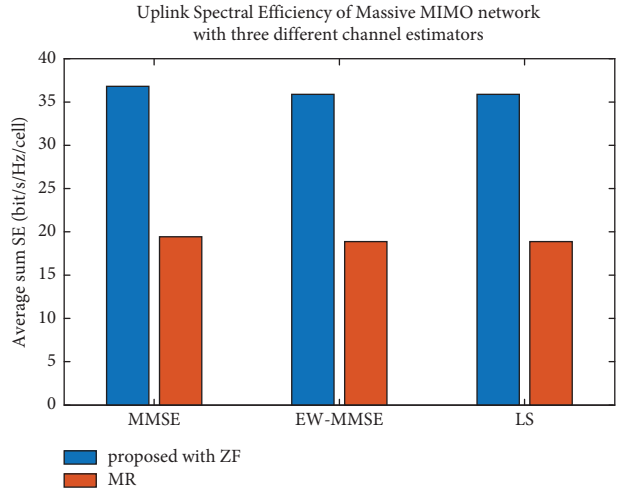

Figure 12: Average UL sum SE of multicell massive MIMO network when using MMSE, EW-MMSE LS channel estimators, and a pilot reuse factor of $f = 1$, using the ZF uplink combining scheme.

Figure 12 shows the uplink spectral efficiency of multicell massive MMIMO network using MMSE, EW-MMSE, and LS channel estimators with zero forcing uplink combining and a pilot reuse factor of $f = 1$. As shown in figure, the uplink spectral efficiency of MMSE-ZF for a pilot reuse factor of $f = 1$ is 38 bit/s/Hz/cell and for EW-MMSE-ZF with pilot reuse factor of $f = 1$ is 36 bit/s/Hz/cell and for LS-ZF with a pilot reuse factor of $f = 1$ is 36 bit/s/Hz/cell.

5. Conclusions

In this paper, the UL spectral efficiency with the MMSE, EW-MMSE, and LS and the pilot reuse factor (i.e., $f = 1, 2, 3$) with uplink ZF combining are analyzed. The expression of uplink spectral efficiency of each channel estimator is derived to model the behaviour under the Rician fading channel. Through simulations, we analyzed the effect of SNR value, code block length, number of UEs, and BS antenna numbers. It is concluded that the multicell, massive MIMO networks considering an efficient pilot reuse factor and highly qualified channel estimator have achieved the enhanced spectral efficiency and area throughput. The MMSE and ZF uplink combining are found to be more suitable in improving SE as compared to MMSE-MR. In addition, SE depends on the number of UEs within cells. It becomes saturated for number of UEs ranging 145, 181, and 155 for the given pilot reuse factors. However, there is not much effect on coherence block as when it increases, then the SE increases as well. It is also observed based on results that the ZF uplink combining technique can suppress the coherence interference and hence the average sum SE is enhanced with MMSE channel estimator and a pilot reuse factor of $f = 3$ with ZF uplink combining. In additional, the results indicate that the uplink spectral efficiency of multicell massive MIMO networks for a pilot reuse factor $f = 3$ has a better performance than the other pilot reuse factors $f \in \{1, 4\}$ with a considerable number of UEs, SNR values, code block length, and BS antenna numbers.

Data Availability

The data used to support the findings of the study are available from the corresponding author upon reasonable request.

Conflicts of Interest

The authors declare that there are no conflicts of interest.

References

[1] S. A. Khwandah, J. P. Cosmas, P. I. Lazaridis, Z. D. Zaharis, and I. P. Chochliouros, "Massive MIMO Massive MIMO Systems for 5G Communicationsystems for 5G communications," *Wireless Personal Communications*, vol. 120, no. 3, pp. 2101–2115, 2021.

[2] A. Misso, M. Kissaka, and B. Maiseli, "Exploring pilot assignment methods for pilot contamination mitigation in massive MIMO systems," *Cogent Engineering*, vol. 7, no. 1, Article ID 1831126, 2020.

[3] Ö. Özdogan, E. Björnson, and E. G. Larsson, "Massive MIMO with spatially correlated Rician fading channels," *IEEE Transactions on Communications*, vol. 67, no. 5, pp. 3234–3250, 2019.

[4] I. Khan, J. J. P. C. Rodrigues, J. Al-Muhtadi et al., "A robust channel estimation scheme for 5G massive MIMO systems," *Wireless Communications and Mobile Computing*, vol. 2019, Article ID 3469413, pp. 1–8, 2019.

[5] E. Björnson, J. Hoydis, and L. Sanguinetti, "Massive MIMO networks: spectral, energy, and hardware efficiency," *Foundations and Trends in Signal Processing*, vol. 11, no. 3-4, pp. 154–655, 2017.

[6] M. A. M. Moqbel, W. Wangdong, and A.-M. Z. Ali, "MIMO channel estimation using the LS and MMSE algorithm," *IOSR Journal of Electronics and Communication Engineering*, vol. 12, no. 1, pp. 13–22, 2017.

[7] R. Chataut and R. Akl, "Massive MIMO systems for 5G and beyond networks—overview, recent trends, challenges, and future research direction," *Sensors*, vol. 20, no. 10, p. 2753, 2020.

[8] R. M. Asif, M. Shakir, A. U. Rehman, M. Shafiq, R. A. Khan, and W. U. Khan, "Performance evaluation of spectral

efficiency for uplink and downlink multi-cell massive MIMO systems," *Journal of Sensors*, vol. 2022, Article ID 7205687, 12 pages, 2022.

[9] W. A. Ali, W. R. Anis, and H. A. Elshenawy, "Spectral efficiency enhancement in Massive MIMO system under pilot contamination," *International Journal of Communication Systems*, vol. 33, no. 8, p. 4342, 2020.

[10] V. Saxena, G. Fodor, and E. Karipidis, "Mitigating pilot contamination by pilot reuse and power control schemes for massive MIMO systems," in *Proceedings of the int conf. on IEEE 81st Vehicular Technology Conference (VTC Spring)*, pp. 1–6, Glasgow, Scotland, May 2015.

[11] M. A. Hosany, "Efficiency analysis of Massive MIMO systems for 5G cellular networks under perfect CSI," in *Proceedings of the 3rd International Conference on Emerging Trends in Electrical, Electronic and Communications Engineering (ELECOM)*, pp. 34–39, Balaclava, Mauritius, November 2020.

[12] L. Sanguinetti, E. Björnson, and J. Hoydis, "Toward massive MIMO 2.0: understanding spatial correlation, interference suppression, and pilot contamination," *IEEE Transactions on Communications*, vol. 68, no. 1, pp. 232–257, 2020.

[13] Y. S. Cho, J. Kim, W. Y. Yang, and C. G. Kang, *MIMO-OFDM Wireless Communications with MATLAB*, John Wiley & Sons, Hoboken, NJ, USA, 2010.

[14] J. Zhang, H. Deng, Y. Li, Z. Zhu, G. Liu, and H. Liu, "Energy Energy Efficiency Optimization of Massive MIMO System with Uplink Multi-Cell Based on Imperfect CSI with Power Controlfficiency optimization of massive MIMO system with uplink multi-cell based on imperfect CSI with power control symmetry," *Symmetry*, vol. 14, no. 4, p. 780, 2022.

[15] A. Ali, I. Ali, A. Latif, S. Ali, and E. Saba, "Spectral efficiency of massive MIMO communication systems with zero forcing and maximum ratio beamforming," *International Journal of Advanced Computer Science and Applications*, vol. 9, no. 12, 2018.

[16] G. M. Zebari, D. A. Zebari, and A. Al-zebari, "Fundamentals of 5G cellular networks: a review," *Journal of Information Technology and Informatics*, vol. 1, no. 1, pp. 1–5, 2021.

[17] M. I. Zahoor, Z. Dou, S. B. H. Sh ah, I. U. Khan, S. Ayub, and T. Reddy Gadekallu, "Pilot decontamination using asynchronous fractional pilot scheduling in massive MIMO systems," *Sensors*, vol. 20, no. 21, Article ID 6213, 2020.

[18] J. He, J. Zhang, C. Song, and M. Wu, "Spectral Spectral Efficiency of the Multiway Massive System over Rician Fading Channelsfficiency of the multiway massive system over rician fading channels," *Security and Communication Networks*, vol. 2021, Article ID 6618363, 8 pages, 2021.

[19] P. Kaur and R. Garg, "A survey on key enabling technologies towards 5G," in *Proceedings of the IOP Conference Series: Materials Science and Engineering*, Chandigarh, India, August 2021.

[20] P. Krishna, T. A. Kumar, and K. K. Rao, "A review on importance of improving spectral efficiency in massive MIMO communications," in *Proceedings of the National Conference on Computer Security, Image Processing, Graphics, Mobility and Analytics (NCCSIGMA)*, Telangana, India, December 2016.

[21] F. Hu, K. Wang, S. Li, and L. Jin, "Energy efficiency-oriented resource allocation for massive MIMO systems with separated channel estimation and feedback," *Electronics*, vol. 9, no. 4, 582 pages, 2020.

[22] Y. Xin, P. Shi, X. Xia, and X. Fan, "Spectral efficiency analysis of multi-cell multi-user massive MIMO over channel aging," *IET Communications*, vol. 14, no. 5, pp. 811–817, 2020.

[23] X. Wang, H. Hua, and Y. Xu, "Pilot-Pilot-Assisted Channel Estimation and Signal Detection in Uplink Multi-User MIMO Systems With Deep Learningssisted channel estimation and signal detection in uplink multi-user MIMO systems with deep learning," *IEEE Access*, vol. 8, pp. 44936–44946, 2020.

[24] J. Li, D. Wang, P. Zhu, and X. You, "Energy efficiency optimization of distributed massive MIMO systems under ergodic QoS and per-RAU power constraints," *IEEE Access*, vol. 7, pp. 5001–5013, 2019.

[25] K. Vasudevan, K. Madhu, and S. Singh, "Data Data Detection in Single User Massive MIMO Using Re-Transmissionsetection in single user massive MIMO using Re-transmissions," *The Open Signal Processing Journal*, vol. 6, no. 1, pp. 15–26, 2019.

[26] K. Vasudevan, S. Singh, and A. Phani Kumar Reddy, *Coherent Receiver for Turbo Coded Single-User Massive MIMO-OFDM with Retransmissions*, IntechOpen, London, UK, 2019.

[27] K. Vasudevan and A. Phani Kumar Reddy, "Gyanesh kumar pathak and mahmoud albreem, "turbo coded single user massive MIMO"," *Sensors & Transducers*, vol. 252, no. 5, pp. 65–75, 2021.